Applied Chemical Engineering (2026) Volume 9 Issue 3 ISSN: 2578-2010 (O)
doi: 10.59429/ace.v9i3.5899

RESEARCH ARTICLE

DFT Calculations for An Organic Structures Based on Anthracene

Ghufran Mohammed Hasan Obaid*, Basim abdullattef ghalib

Laser Physics Department, College of Science for Women, University of Babylon, Hilla, IRAQ

***Corresponding author:** Ghufran Mohammed Hasan Obaid, ghm681292@gmail.com

ABSTRACT

B3LYP hybrid functional DFT was used with 6-31G basis sets for calculating the ground state properties of anthracene and its derivatives. The optimized structures were obtained from the used method after only two steps of optimization. The LUMO-HOMO gap for the reference anthracene was reduced 0.91 eV by adding di-amine and thiophene and construct structure 3. The new suggested structures based on anthracene are more electronic softness and less hard compared with anthracene. High electronic softness means the structure more reactive in which the softness is willingness to accept electrons. Structure 3 has high degeneracy of molecular orbital in comparison with the others. The new suggested structures offer an advantage in charge transfer compared to anthracene. The map of electrostatic potential and total charge density showed the active areas of high negativity are localized in sulfur in thiophene and di-amine and this give these structures high activity to interact with other species. UV-Vis spectrum showed direct transition from valence band to conduction band, this makes these structures ideal systems for use in optical devices, such as, photodetector, solar cell, and light emitted diode LED and laser diode, and indirect transition with different values of probability depending on the wave length of each spectrum and this make the structures can be used for many application, such as, transistors, rectifiers and filters as optical applications.

Keywords: Anthracene, HOMO, LUMO, DOS, ESP and UV-Vis.

ARTICLE INFO

Received: 03 February 2026
Accepted: 06 May 2026
Available online: 01 July 2026

1. Introduction

Anthracene is a polycyclic aromatic hydrocarbon (PAH) made up of three interconnected benzene rings set in a linear arrangement. The three benzene rings are fused together, sharing two carbon atoms at each junction[1, 2]. This leads to a continuous conjugated system that improves its capacity to conduct electricity and absorb light. Anthracene's carbon atoms are sp2 hybridized, creating a network of double bonds (C=C) and single bonds (C-C). The resonance structure generated by the alternating double bonds enhances the molecule's stability. The chemical formula of anthracene is C14H10, which allows for effective π - π stacking interactions between molecules. This planarity contributes to its electronic properties and stability[2, 3]. The characteristic feature of anthracene is its facile photochemistry, most notably the Diels-Alder reaction with singlet oxygen or dienophiles and its ability to undergo photo dimerization. These reactions allow for reversible chemical manipulation, which is essential for photo-switchable materials and chemical trapping agents. The growing need for effective and adaptable synthetic methods has led chemists to investigate novel ways to create anthracene derivatives, especially using transition metal catalysis uses in different domains, such as organic electronics, photovoltaics, and medicinal chemistry[3-5].

Anthracene shows significant absorption in the ultraviolet-visible (UV-Vis) spectrum, peaking at a wavelength of approximately 254 nm. Its high fluorescence quantum yield makes it a super candidate for light-emitting applications[6].

Thiophene is a fundamental and highly important aromatic heterocyclic compound with the molecular formula C4H4S. It consists of a planar, five-membered ring containing four carbon atoms and one sulfur atom. Thiophene has since become an indispensable building block in organic synthesis, materials science, and medicinal chemistry fabrication of light-emitting diodes in material science[7-9]. Thiophene is soluble in most organic solvents but insoluble in water. Its sulfur atom contributes delocalized electron pairs to the π -system, giving thiophene high aromatic stability and reactivity comparable to benzene, with closely similar physicochemical properties[10].

2. Computation Methods

Density functional theory (DFT) is the most effective approach to compute the electronic structure of matter. It foresees an excessive variety of molecular properties and derives properties of a many-particle system as an electron density functional[11].

Time-dependent density functional theory (TD-DFT) can be used to look at the excited-state properties of a system in being there of time-dependent potentials. The power of TD-DFT show an important for computing excitation energies, oscillator strength, wavelength, molecular orbital character and electronic transitions.

The relax structure of CNR was obtained from Berney algorithm[12-14]. Becke exchange function (B)[15] and the functional Becki-adiabatic compound three-parameter hybrid binding (B3)[15, 16] were used in combine with the correlation function Lee-Yang par B3LYP[15]. To solve Kohn-Sham equations, 6- 31G double Zeta polarization DZP were used for orbital spread. The calculated the points of stationary, meant for the configurations and strength fields are displayed, match up to actual least on the hyperactive outsides of the potential molecular energy. Energy gap for a single molecule examined here was calculated on the similar theoretical level. Gaussian 09 package of program was used for computing all the ground and excited states calculations[14].

The two most major of molecular orbitals are frontier orbitals as they lie at the limitations of the electrons of the molecule. They are: the highest occupied molecular orbital HOMO as orbital performing by means of an electron donating, and the lowest unoccupied molecular orbital LUMO is taking place for accepting electrons. Energy band gap can be computing as the distance between the two edges of HOMO and LUMO[16-19]:

$$E_{gap} = E_{LUMO} - E_{HOMO} \qquad (1)$$

The path of molecules that interacts with other species did not determining only by terms of HOMO and LUMO, and corresponding energy gap, but the energy gap of the molecules supports the chemical activity for a molecule.

Global electrochemical hard-ness (H) is the amount of resistance for a molecule to vary or distortion, _takes the formula[15]:

$$H = \frac{IE-EA}{2} \qquad (2)$$

Where IE and EA are the ionization energy and electron affinity, respectively.

The electronic softness (S) of a molecule is associated with the energy gap that the molecule possesses. The soft molecules have a small energy gap and this means small excitation energies to the several of excited states, their electron density changes more simply than hard molecules, therefore, molecules with highly soft-

ness are further responsive than molecules with highly hard-ness. Electronic soft-ness is a characteristic for molecules that dealings the degree of electro-chemical activity. It is the inverse of (H)[15]:

$$S = \frac{1}{2H} \qquad (3)$$

The Electrophilic Index (ω) quantifies a molecule’ s ability to accept electron density, calculated as[15]:

$$\omega = \frac{\chi^2}{2H}$$

Where x the electronegativity of the molecule, can be calculated as in below formula[15]:

$$\chi = \frac{IE + EA}{2}$$

3. Results and discussion

Figure 1 shows the optimal structure for anthracene as a reference molecule and two of its derived structures. The three studied structures were relax to minimum ground state energy and symbolled 1, 2 and 3. The full steps of optimization for the three structures under study to reach the lowest energy value for the structures were relied on solving the equations of self-consistent field SCF and therefore depend on the number of iteration for each cycle, SCF relates to quantity of electrons in each structure. The relationship between the number of optimization steps and the minimum energy for the studied structures is illustrated in figure 2. Above relationship showed that the ground state energy for the studied structures was calculated approximately after two steps without any imaginary frequency and this indicate to good appropriate choice of basis sets to describe the atomic orbitals in each structure.

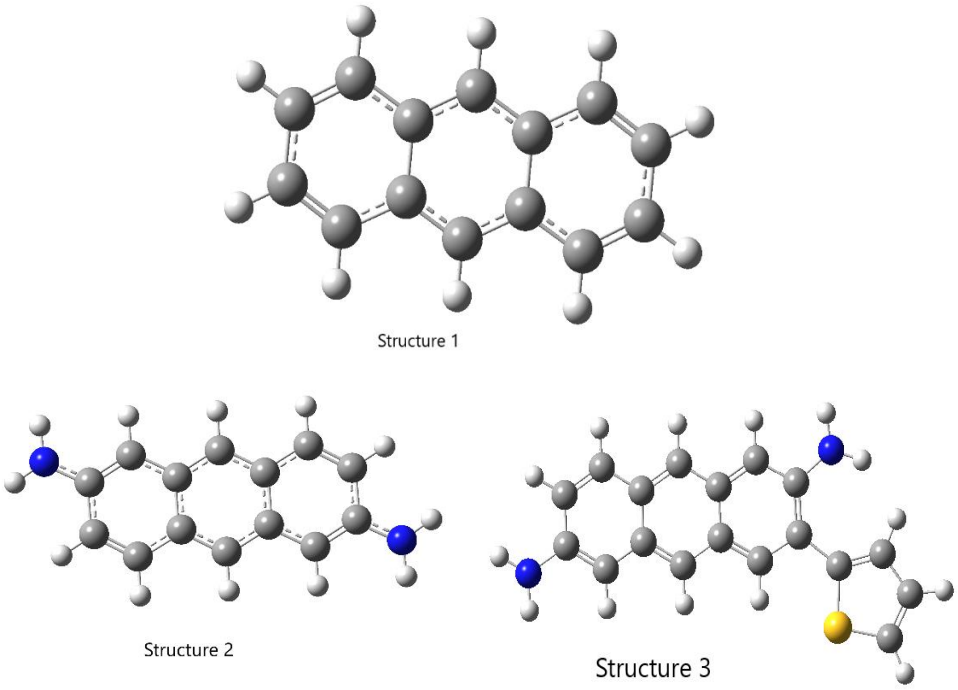

Figure 1. Optimized structures under study from the SCF.

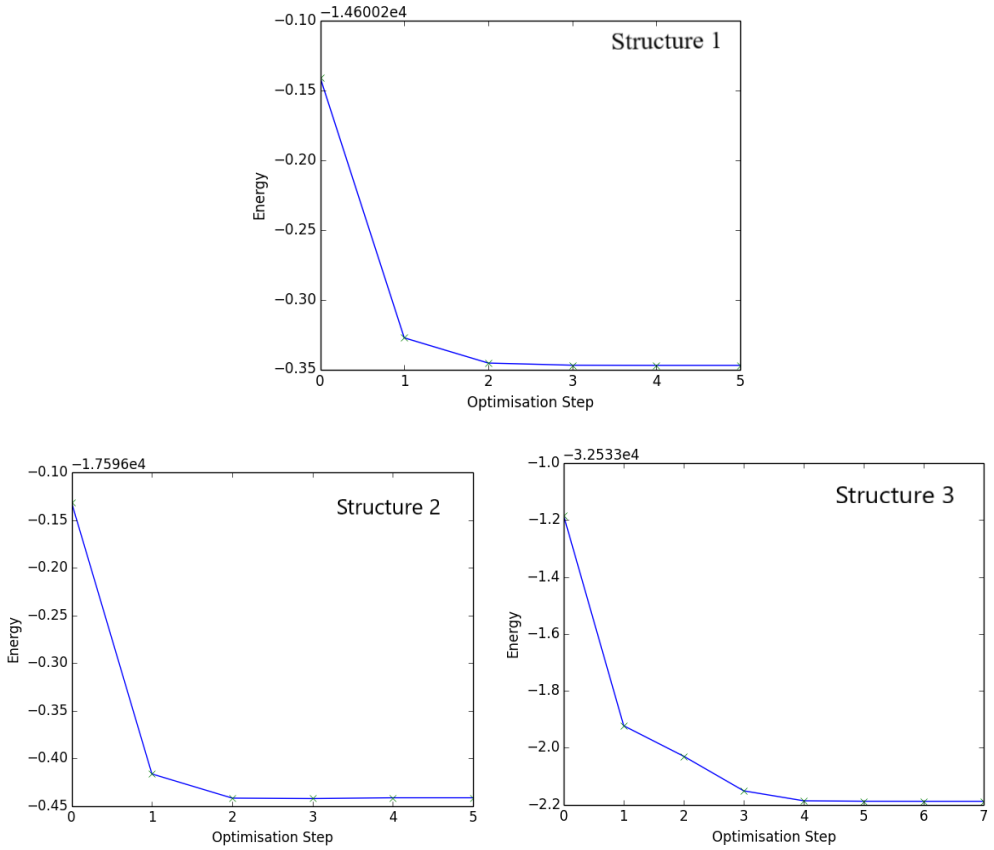

Figure 2. Total energy in a. u as a function of optimized steps for the studied structures.

Table 1 illustrates the results of High Occupied Molecular Orbital Energy EHOMO, Lowest Unoccupied Molecular Orbital ELUMO, and Energy gap Egap for the three structures. As shown in table 1, the electronic properties of anthracene molecule have been affected by the addition of terminal groups to the molecule. Anthracene has an energy gap of (3.6906 eV), and when NH2 is added in the two ends of anthracene, its energy gap becomes (3.1717 eV). This indicates a change in the electronic properties of the reference molecule. When a thiophene molecule is added to structure 2, we observe that the energy gap decreases to (2.7757 eV), which means obtaining a new structure that can be used in many electronic applications. Figure 3 illustrates the HOMO, LUMO and energy gap for the structures under study.

Table 1. Energies of HOMO, LUMO, and Energy gap for the studied structures.

Structure	E_{HOMO} **(eV)**	E_{LUMO} **(eV)**	E_{gap} **(eV)**
1	-5.348	-1.657	3.6906
2	-4.1774	-1.0057	3.1717
3	-4.28845	-1.51265	2.7757

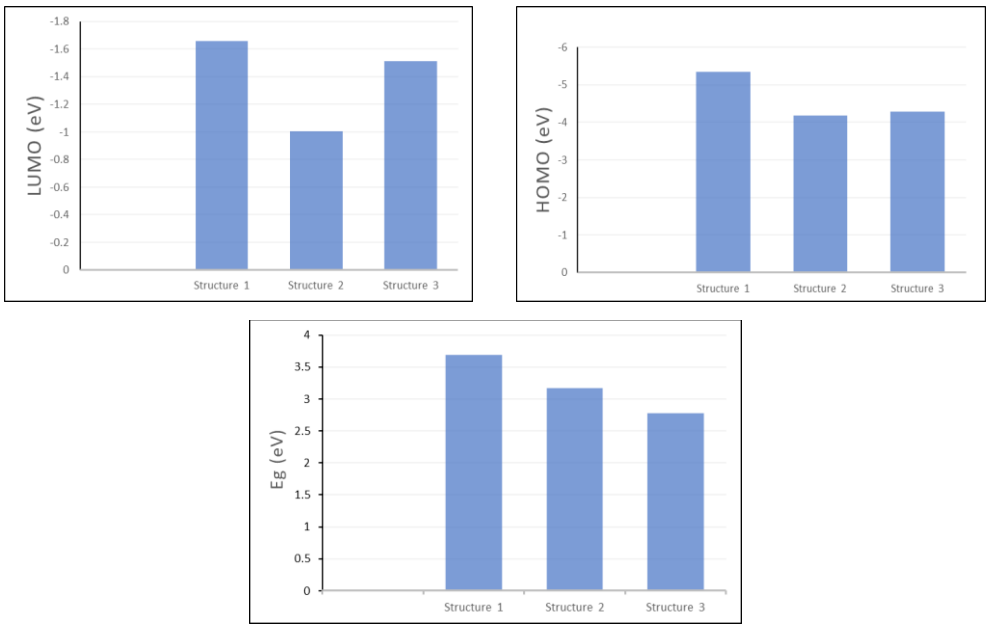

Figure 3. HOMO, LUMO and Eg for the studied structures.

The distribution of wave functions represented by the shapes of HOMO and LUMO for the three structures under study is illustrated in Figure 4. These shapes are resultant from the linear combination of atomic orbitals contributed to form the molecular orbitals LCAO-MO in each structure. In figure 4, the green color represents the positive charges and the red represents the negative charges. The distribution of the positive and negative charges is due to symmetry for each structure, structure 1 (anthracene) has high symmetrical distribution due to present the aromatic benzene molecules. On the other hand, there is no contribution from the thiophene molecule in the HOMO of structure 3, while it does contribute to the LUMO. In general, structure 3 has asymmetric distribution of LUMO comes from the presence of a sulfur atom in thiophene.

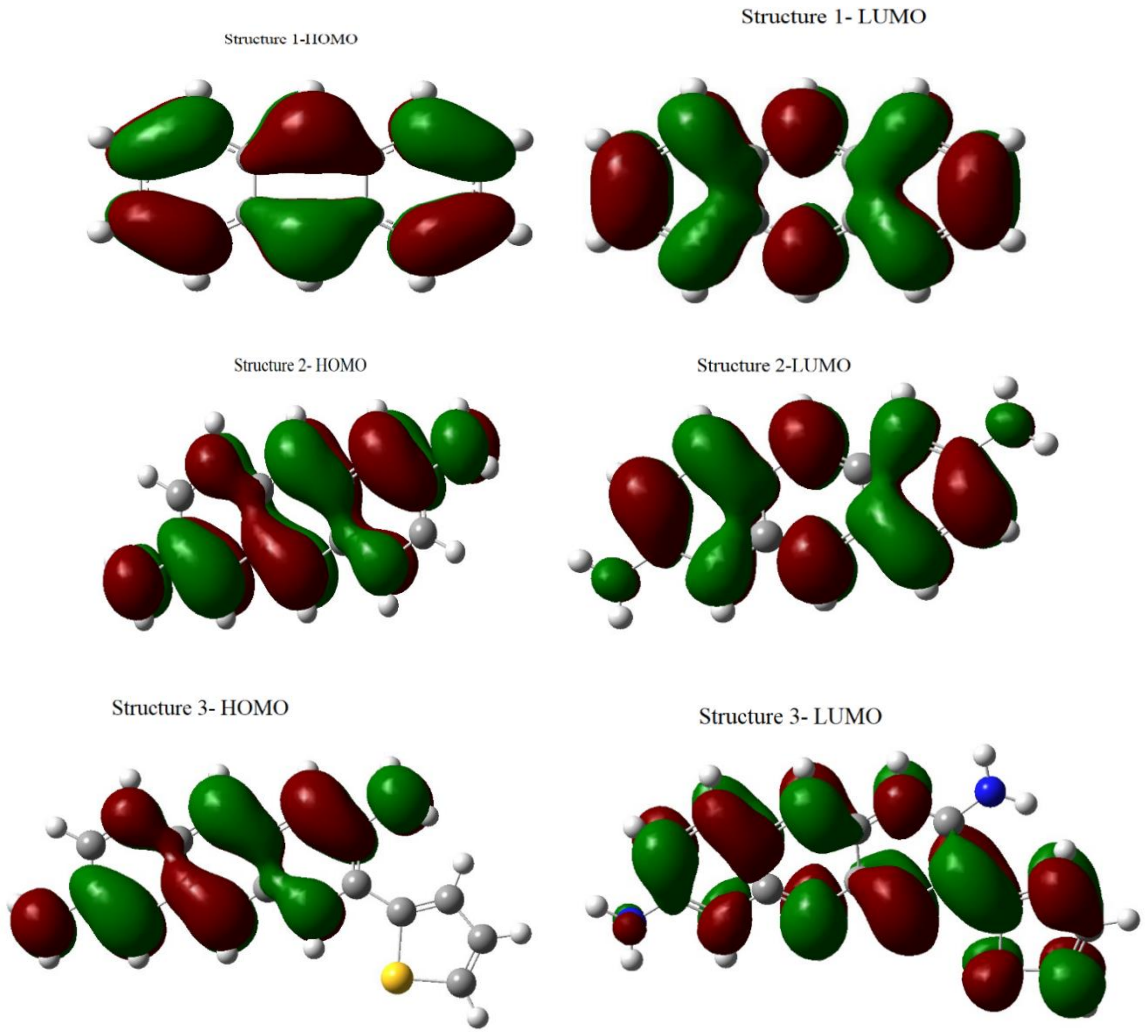

Figure 4. HOMO and LUMO shapes for the studied structures.

Table 2 shows the results of Ionization Energy IE, Electron Affinity EA, Electronic Softness S, Hardness H and Electrophilic Index ω for the studied structures obtained using the Koopmans method.

Table 2. IE, EA, S, H and ω for the studied structures.

Structure	IE (eV)	EA (eV)	S (eV)	H (eV)	ω (eV)
1	5.3475	1.6569	0.2709	1.8453	3.3234
2	4.1774	1.0057	0.3152	1.5858	2.1175
3	4.2884	1.5126	0.3602	1.3879	3.0308

According to Koopmans theorem, the calculated values of IE and EA for anthracene are 5.3475 eV and 1.6569 eV, respectively. This means that the reference (structure 1) needs a high amount of energy to donating an electron. Adding the di-NH2 in the ends of anthracene to construct the structure 2 leads to decrease these values to 4.1774 eV and 1.0057 eV for. The values of IE and EA for structure 3 are 4.2884 eV and 1.5126 eV, respectively, and these results indicate to high ability for structure 3 to donating an electron, or it needs low energy to donate an electron from the molecule and becomes anion.

Returning to table 2, we find that the electronic softness is inversely proportional to electronic hardness for all the studied structures, Structure 3 is has high softness and less hardness comparing with the others, that means, it has high ability to allow the electrons to transfer to other surrounding species. Above results refer to that the two suggested structure 2 and structure 3 can play role in many electronic application in optoelectronic devices. Regarding Electrophilic Index, all structures have good value of ω and they can acceptance of bonding with other atoms, molecules, or structures and this makes these structures important in many different electronic applications.

Figure 5 declares the Density of States DOS for the anthracene molecule and its derive drawn from the calculations of the SCF-DFT by employing the B3LYP hybrid functional. The figure showed the number of degeneracy of occupied orbitals in all structures are more than that of unoccupied orbitals, but the rank of degeneracy of molecular orbital is as: structure 3 > structure 2 > structure 1. The new suggested structures offer an advantage in charge transfer compared to a reference anthracene molecule.

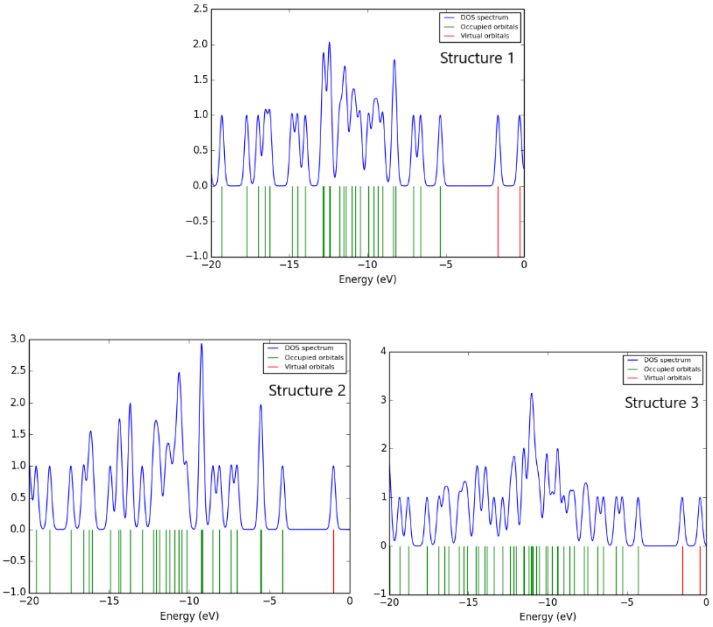

Figure 5. DOS spectra for the studied structures.

Figure 6 shows the behavior of the electrostatic potential ESP for the structures under study. One can declares from mentioned figure the potential was symmetrically distributed in the reference structure (anthracene molecule) due to high symmetric of the three benzene molecule that construct the anthracene structure. As known, ESP imagines how charge is distributed on a molecule surface, the difference in map of ESP distribution regions demonstrating where it's probable to attract or resist other molecules or components, central for expecting reactivity, drug binding, and molecular interactions in the many fields, such as, physics, chemistry and drug design. In structure 3, the charge was highly dragged towards the sulfur atom in thiophene molecule. Above result can be give an idea about the types of molecules containing atoms of highly electronegativity that added in contact to the surface of the structures under study.

The behavior of the charge density of the structures under study is likely to that of electrostatic potential, in which the map of total charge density for anthracene showed the charge is distributed uniformly due to high symmetry that the anthracene has. While the two other structures showed distribution of total charge density depending on the present of atoms of highly negativity. In structure 3, the distribution declare the charge was dragged towards the sulfur atom in thiophene and towards the di-amine in structure 3 because the electronegativity of nitrogen attracts electron density towards itself, as seen in figure 7.

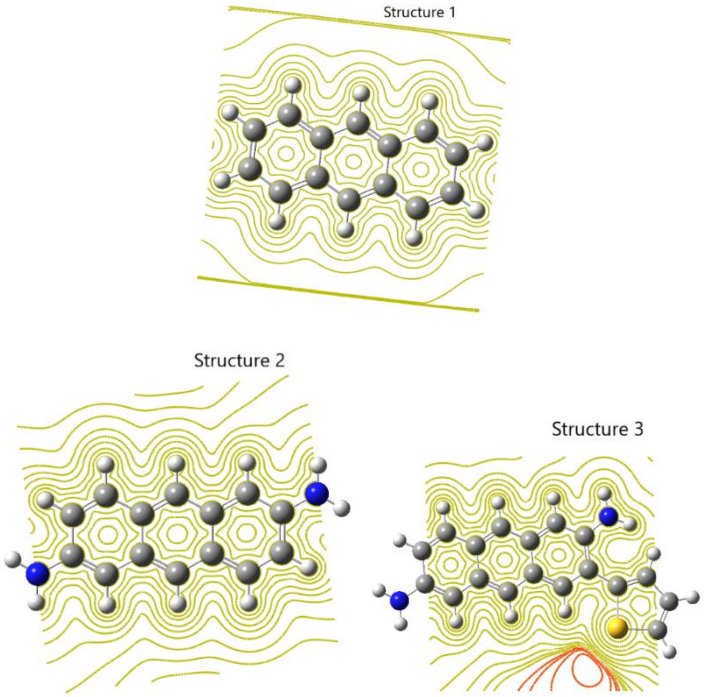

Figure 6. Distribution of ESP for the studied structures.

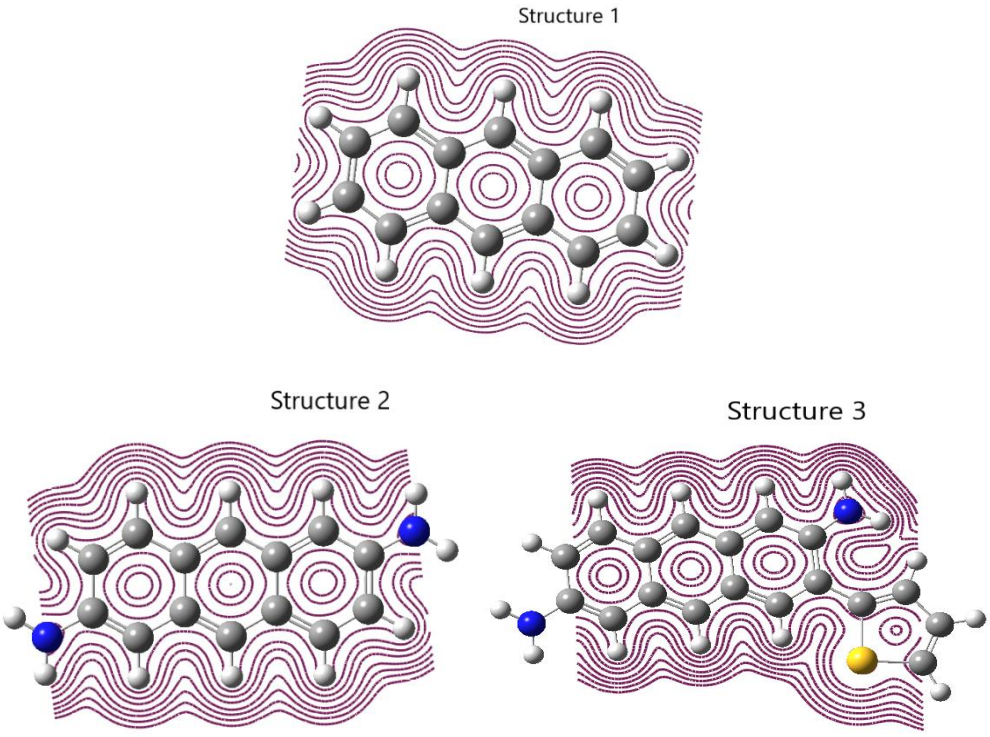

Figure 7. Map of total charge density Distribution for the studied structures.

TD-DFT method was used to investigate the electronic transitions for the studied structures. Tables 3 declares the values of excitation energy, corresponding wave length, oscillation strength for each spectrum and transition states. The observed transition states for the structures involves both direct transition from valence band to conduction band and indirect transition with different values of probability depending on the wave length of each spectrum. This result make from these structures play a significant role in many electronic

applications. As known, the direct transition makes these structures ideal systems for use in optical devices, such as, photodetector, solar cell, and light emitted diode LED and laser diode. On the other hand, the indirect transitions qualify these structures for many application, such as, transistors, rectifiers and filters as optical applications. Figure 8 illustrates the UV-Vis spectrum for the studied structures.

Table 2. Excitation energy, wave length, oscillation strength and transition states for the structures.

Complexes	Excitation Energy (eV)	Wave Length (nm)	Oscillator Strength	Transitions HOMO→LUMO
Structure 1	3.4202	362.51	0.0651	(HOMO→ LUMO (98%))
	4.0242	308.10	0.0018	H-1→LUMO(53%) HOMO→L+1(47%)
	4.7198	262.69	0.000	H-2L→UMO(68%) HOMO→L+2(32%)
Structure 2	2.8451	435.78	0.0822	HOMO→LUMO(97%)
	3.9159	316.62	0.004	H-1→L(60%),H→L+1(37%)
	4.0017	309.83	0.0000	H-2→L(93%),H>L+2(5%)
Structure 3	2.3865	519.52	0.0413	HOMO→LUMO(98%)
	3.4099	363.60	0.1198	H-1→L(61%) H→L+1(34%)
	3.5974	344.65	0.2778	H-2→L(33%), H-1→L(15%),H→L+1(45%) H→L+2(6%)

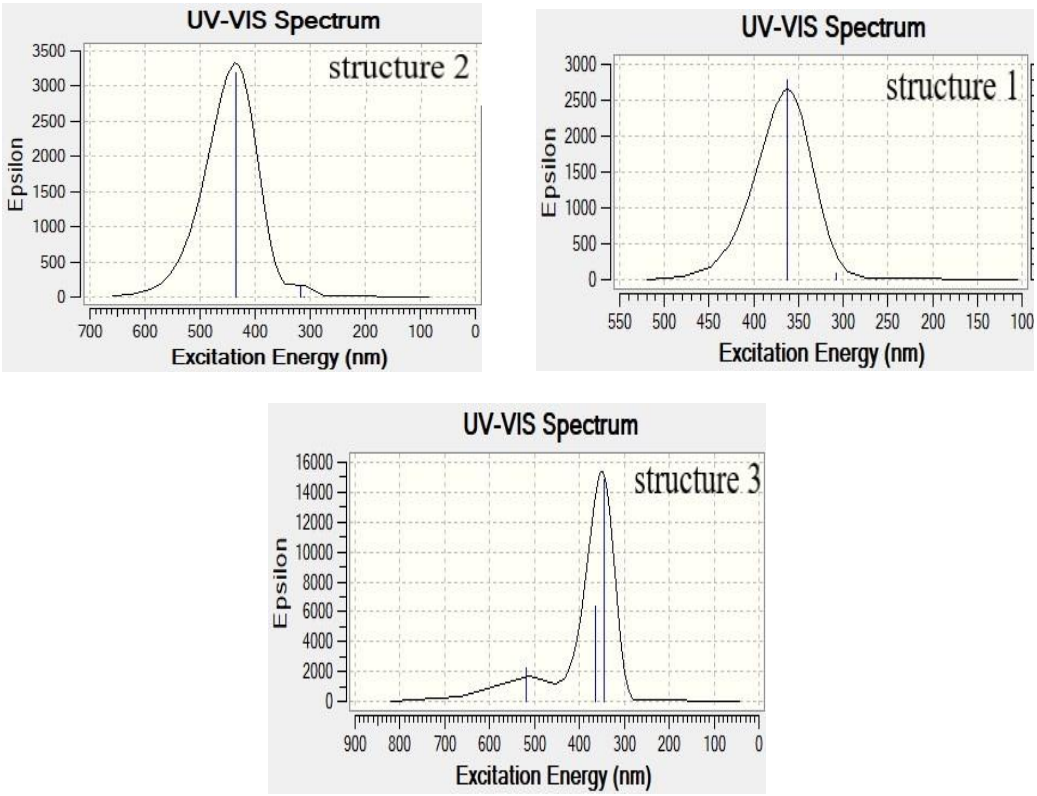

Figure 8. UV-Vis spectrum for the studied structures.

4. Conclusion

B3LYP hybrid functional with 6-31G basis sets is a good choice for the ground state calculations for anthracene and its derivatives. The optimization for the studied structures was satisfy after only two steps of

iteration in used DFT method. The LUMO-HOMO gap for anthracene was reduced 0.91 eV by adding the thiophene with di-amine in structure 3. The new suggested structures based on anthracene are more electronic softness and less hard compared with anthracene. High electronic softness means the structure more reactive in which the softness is willingness to accept electrons. Number of degeneracy of occupied orbitals in all structures are more than that of unoccupied orbitals, structure 3 has high degeneracy of molecular orbital in comparison with the others. The new suggested structures offer an advantage in charge transfer compared to anthracene. The map of electrostatic potential and total charge density showed the active areas of high negativity are localized in sulfur in thiophene and di-amine. UV-Vis spectrum showed direct transition from valence band to conduction band, this makes these structures ideal systems for use in optical devices, such as, photodetector, solar cell, and light emitted diode LED and laser diode, and indirect transition with different values of probability depending on the wave length of each spectrum and this make the structures can be used for many application, such as, transistors, rectifiers and filters as optical applications.

References

1. Bass, A. D., Castellanos, D., Calicdan, X. A., & Cao, D. D. (2024). Synthesis and characterization of 1, 2, 3, 4-naphthalene and anthracene diimides. Beilstein Journal of Organic Chemistry, 20(1), 1767-1772.
2. Aydemir, M., Haykir, G., Selvitopi, H., Yildirim, O. C., Arslan, M. E., Abay, B., & Turksoy, F. (2023). Exploring the potential of anthracene derivatives as fluorescence emitters for biomedical applications. Journal of Materials Chemistry B, 11(19), 4287-4295.
3. Shi, W., Yang, X., Li, X., Meng, L., Zhang, D., Zhu, Z., ... & Zhao, D. (2022). Syntheses of anthracene‐centered large PAH diimides and conjugated polymers. Chemistry–A European Journal, 28(24), e202104598.
4. Khandaka, H., Upadhayay, Y., Soni, A., Manoharadas, S., & Joshi, R. K. (2024). Facile synthesis of anthracene-based derivatives via a magnetically retrievable Fe3O4@ SiO2 immobilized selenoether functionalised NHC-Pd (II) heterogenous catalyst: Photophysical, electrochemical and DFT studies of novel 9, 10-anthracene based derivatives. Inorganica Chimica Acta, 565, 121840.
5. Costa, R. F., Oliveira, M. S., Aguiar, A. S., Custodio, J. M., Di Mascio, P., Sabino, J. R., ... & Napolitano, H. B. (2021). Synthesis and structural studies of two new anthracene derivatives. Crystals, 11(8), 934.
6. Sead, F. F., Jain, V., Roopashree, R., Kashyap, A., Saini, S., Chandra Sharma, G., ... & Javahershenas, R. (2025). Recent achievements in synthesis of anthracene scaffolds catalyzed transition metals. Frontiers in Chemistry, 13, 1545252.
7. Mishra, R., Jha, K. K., Kumar, S., & Tomer, I. (2011). Synthesis, properties and biological activity of thiophene: A review. Der Pharma Chemica, 3(4), 38-54.
8. Sumpter, W. C. (1944). The chemistry of isatin. Chemical reviews, 34(3), 393-434.
9. Thakur, S., Kumar, D., Jaiswal, S., Goel, K. K., Rawat, P., Srivastava, V., ... & Dwivedi, A. R. (2025). Medicinal chemistry-based perspectives on thiophene and its derivatives: exploring structural insights to discover plausible druggable leads. RSC Medicinal Chemistry, 16(2), 481-510.
10. Shah, R., & Verma, P. K. (2018). Therapeutic importance of synthetic thiophene. Chemistry Central Journal, 12(1), 137.
11. Jia, X. T.; Campos-Delgado, J.; Terrones, M.; Meunier, V.; Dresselhaus, M. S. Nanoscale (2011), 3, 86–95, " Graphene Edges: A Review of Their Fabrication and Characterization".
12. Zotti G., Schiavon G., Zecchin S., Morin J. F., Leclerc M., Macromolecules. 35 (2002) 2122.
13. Garnier F., Horowitz G., Peng X., Fichou D. , Adv.Mater 2 (1990) 562.
14. E.Gill R., Malliaras G. G., Wildeman J., Hadziioannou G., Adv. Mater 6 (1994) 132.
15. Frisch M.J., Trucks G.W., Schlegel H. B., Scuseria G. E., Robb M.A., Cheeseman J. R., Montgomery J.A., Vreven, T., Kudin, K. N. Jr., Burant, J. C., Millam, J. M., Iyengar, S. S., Tomasi, J., Barone, V., Mennucci, B., Cossi, M., Scalmani, G., Rega, N., Petersson, G. A., Nakatsuji, H., Hada, M, Ehara, M., Toyota, K., Fukuda, R., Hasegawa, J., M.Ishida, Nakajima, T., Honda, Y., Kitao, O., Nakai, H., Klene, M., Li, X., Knox, J. E., Hratchian, H. P., Cross, J. B., Adamo, C., Jaramillo, J., Gomperts, R., Stratmann, R. E., Yazyev, O., Austin, A. J., Cammi, R., Pomelli, C., Ochterski, J. W., Ayala, P. Y., Morokuma, K., Voth, G. A., Salvador, P., Dannenberg, J. J., Zakrzewski, V. G., Dapprich, S., Daniels, A. D., Strain, M. C., Farkas, O., Malick, D. K., Rabuck, A. D., Raghavachari, K., Foresman, J. B., Ortiz, J. V., Cui, Q., Baboul, A. G., Clifford, S., Cioslowski, J., Stefanov, B. B., Liu, G., Liashenko, A., Piskorz, P., Komaromi, I., Martin, R. L., Fox, D. J., Keith, T., Al- Laham, M. A., Peng,

C. Y., Nanayakkara, A., Challacombe, M., Gill, P. M. W., Johnson, B., Chen, W., Wong, M. W., Gonzalez, GAUSSIAN 09, Revision B.04, Gaussian, Inc. Pittsburgh PA. (2009).
16. Becke A. D., J. Chem. Phys. 98 (1993) 5648-5653; Ditchfield R., Hehre W.J., Pople J. A., IX. J. Chem. Phys. 54 (1971) 724-729.
17. Gong X, Zhang Y, Jiang Z, Du C, Khan A and Usman R (2025). Comput Theor Chem 1252:115377. doi: https://doi.org/10.1016/j.comptc.2025.115377.
18. Su W, Jiang Z, Khan A, Usman R and Wang M (2025). Comput Theor Chem 1254:115465. doi: https://doi.org/10.1016/j.comptc.2025.115465.
19. Xu Q, Jiang Z, Gong X, Usman R and Khan A (2026) J Mol Struct 1349:143876. doi: https://doi.org/10.1016/j.molstruc.2025.143876.